PHYSICAL REVIEW B VOLUME 35, NUMBER 4 1 FEBRUARY 1987

Onset of fractal growth: Statics and dynamics of diffusion-controlled polymerization

J. H. Kaufman, A. I. Nazzal, and O. R. Melroy
IBM Almaden Research Center, San Jose, California 95120

A. Kapitulnik
Department of Applied Physics, Stanford University, Stanford, California 94305
(Received 5 May 1986)

We report experimental studies of the statics and dynamics of diffusion-controlled polymerization. The polymerization involves the random aggregation of a neutral precursor, pyrrole monomer, in a two-dimensional electrochemical cell under a variety of conditions. As the oxidation potential is increased, the fractal dimension drops sharply from values near 2 (compact structures) to 1 as the growth becomes dendritic. At higher potentials, where the polymerization becomes diffusion limited, a continuum of structures is observed as the dendrites become more irregular and the fractal dimension increases asymptotically to 1.74 ± 0.01. The mean branch angle is found to decrease sharply from 90° in the dendritic regime to approximately 45° in the diffusion-limited regime. In this regime the width of the active growth zone increases at the same rate as the fractal radius. The spectral dimensionality determined by scale-dependent conductivity measurements is 1.26 ± 0.04.

INTRODUCTION

The apparent universality of scaling behavior characteristic of diffusion-limited aggregation (DLA) has stimulated much interest in random-aggregation phenomenon.[1-6] Theoretical studies and computer simulations[2] have been performed to characterize the class of diffusion-limited aggregates. Experimental studies[3-5] of DLA have successfully determined the Hausdorff-Besicovitch (fractal[6]) dimensionality, D, but have not focused on the conditions necessary for DLA. Moreover, only recently have studies of dynamical properties been performed.[7] In fact, DLA is only the limiting case of a more general process of diffusion-controlled aggregation (DCA). In DCA the free-particle concentration at the growing surface is controlled but not limited by diffusion (see below). Electrochemical deposition provides a unique way to control deposition conditions, in particular the free-particle concentration at the surface. In the present work, we report the preparation of polypyrrole under conditions which vary from diffusion-controlled polymerization (DCP) to diffusion-limited polymerization (DLP). Our goal was to vary the microscopic parameters which lead to DLA and so gain a better understanding of the fundamental processes which affect random aggregation. By varying deposition conditions, we observed a growth instability as structures changed continuously from compact to dendritic to that of a random aggregate. By employing a thin layer cell and appropriate supporting electrolytes, effects of migration and convection were eliminated. Pyrrole was chosen as a precursor for these studies because it is neutral in solution, and because polypyrrole is a poor enough conductor ($10\ \Omega^{-1}\,\mathrm{cm}$) to permit scale-dependent conductivity measurements. Structures of macroscopic size can be obtained [Fig. 1(a)—1(o)], and the polymer is durable enough to be handled and contacted for electrical measurements. Experiments were also performed to demonstrate the importance of screening the electric field in order to adequately control the conditions of aggregation.

THEORY

Diffusion-limited aggregation is a process wherein particles moving in a space with Euclidean dimensionality d undergo a random walk until they interact with (and stick to) a growing fractal.[1,6] By definition, the concentration of aggregating particles near the surface must be sufficiently small such that no interactions occur between them. When an aggregate is produced via DLA, the resultant structure is treelike and self-similar. Because these objects are highly irregular, they cannot be characterized by a single Euclidean dimension. A better description of the structure is provided by the fractal dimension which may be computed from the ensemble average correlation function, $c(r)=r^{-\eta}$, where η, the codimension is given by $D-d$. For random fractals produced by computer simulations on a square lattice, a typical value for the fractal dimension is 1.657 ± 0.004.[1]

A structure grown under diffusion-limited conditions should also exhibit scaling behavior in its dynamic properties.[8-11] For example, the density of states will scale in energy with an exponent D_s known as the spectral dimensionality. This exponent may be obtained from scale-dependent conductivity measurements. Given a fractal structure of finite size, the averaged point to point resistance, ρ, between two electrodes a distance r apart should scale as the separation to a power $\bar{\mu}$ where $\rho\propto r^{\bar{\mu}}$ and $\bar{\mu}\simeq1$ as demonstrated by Witten and Kantor.[10] Stanley and Coniglio[12] proved that $D_s=2D/(D+1)=1.26$ for a fractal without loops and with fractal dimension 1.7. Furthermore, their work demonstrates that the conductivity exponent is one only if there are no loops. The conductivity exponent is actually a direct measure of the chemi-

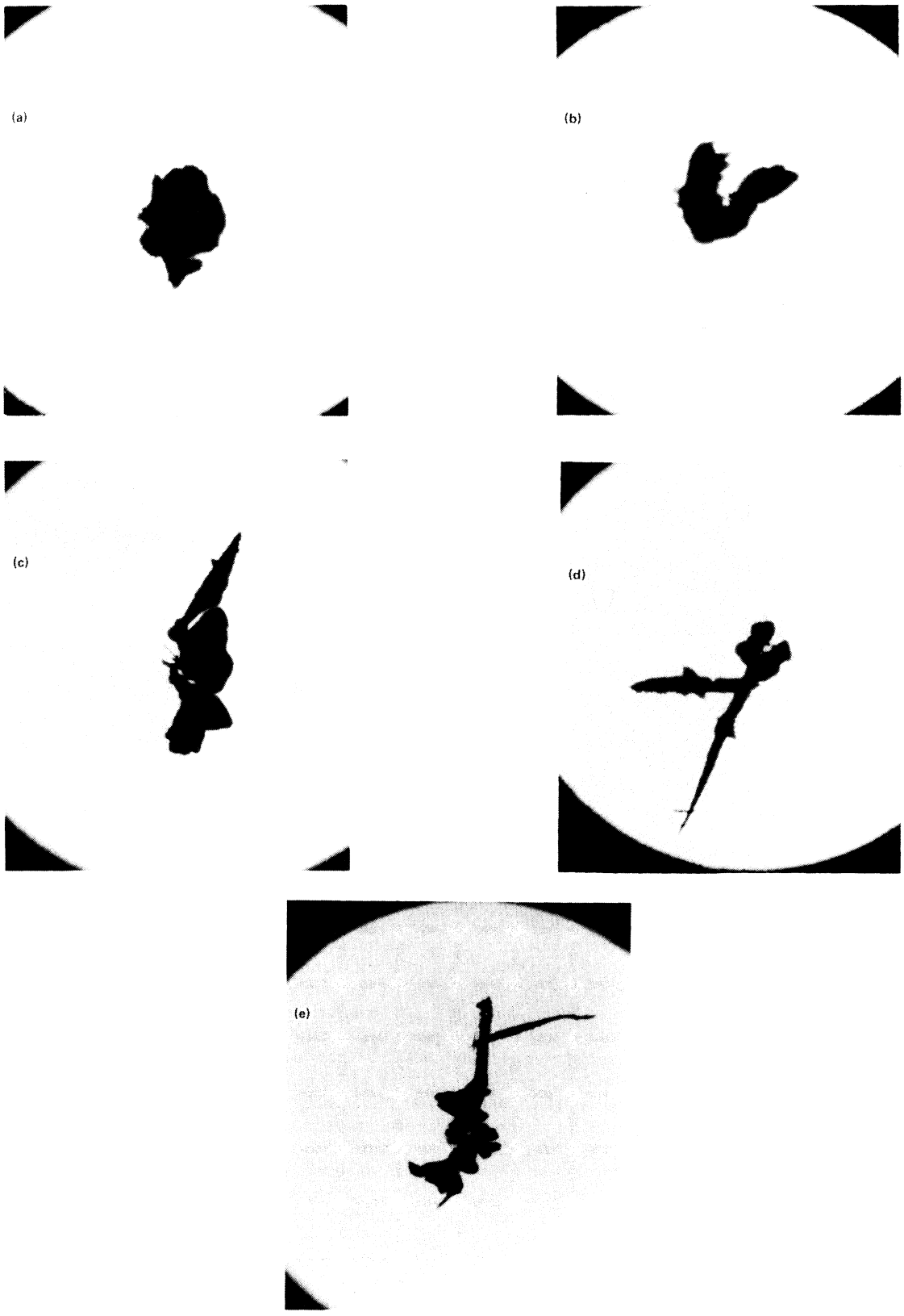

FIG. 1. (a)–(o) Aggregates of polypyrrole prepared via DCP at increasing potential: (a) = 0.8 V; (b) 0.9 V; (c) 1.0 V; (d) 1.1 V; (e) 1.2 V; (f) 1.3 V; (g) 1.4 V; (h) 1.5 V; (i) 1.6 V; (j) 1.8 V; (k) 2.0 V; (l) 3.0 V; (m) 4.0 V; (n) 4.5 V; (o) 6.0 V.

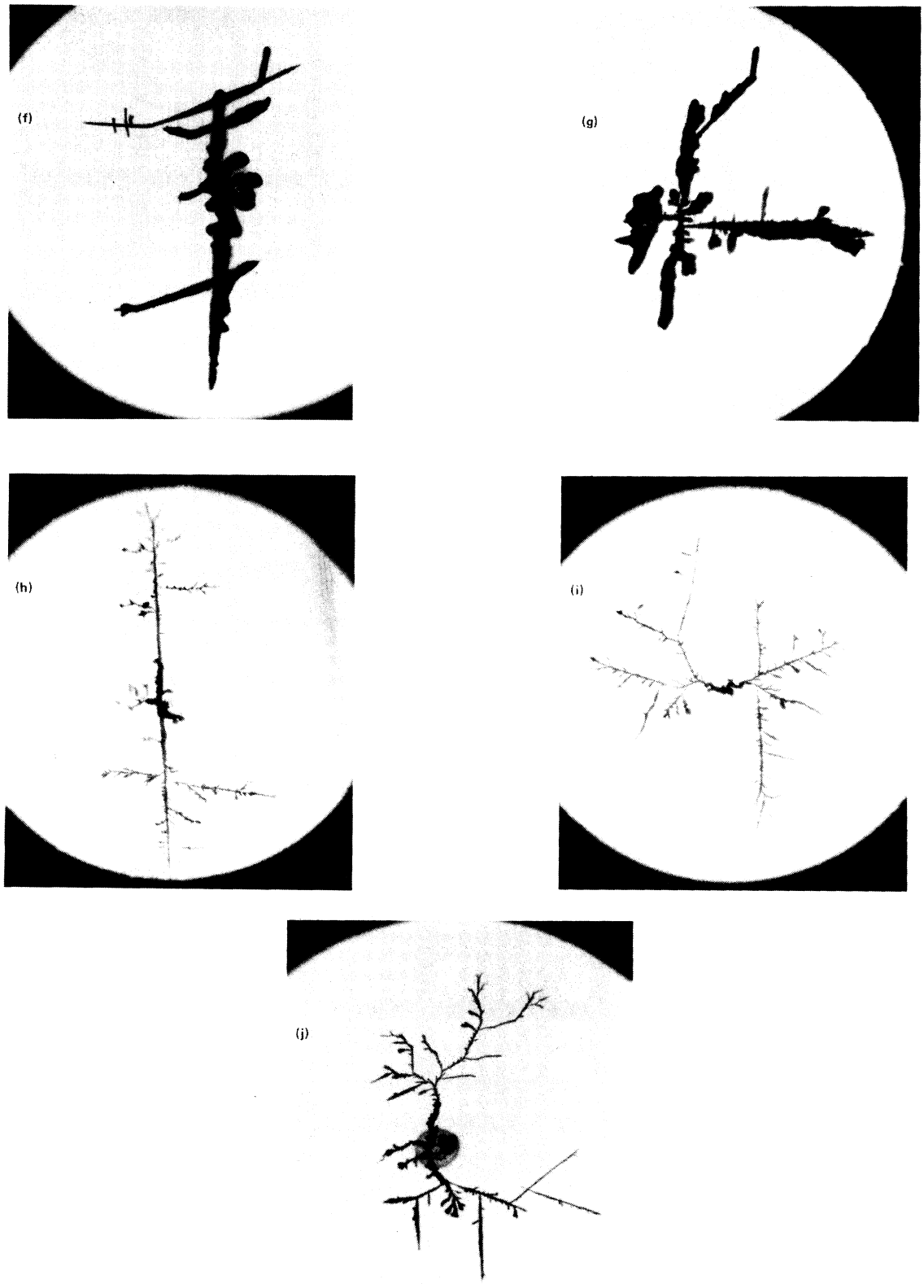

FIG. 1. (*Continued*).

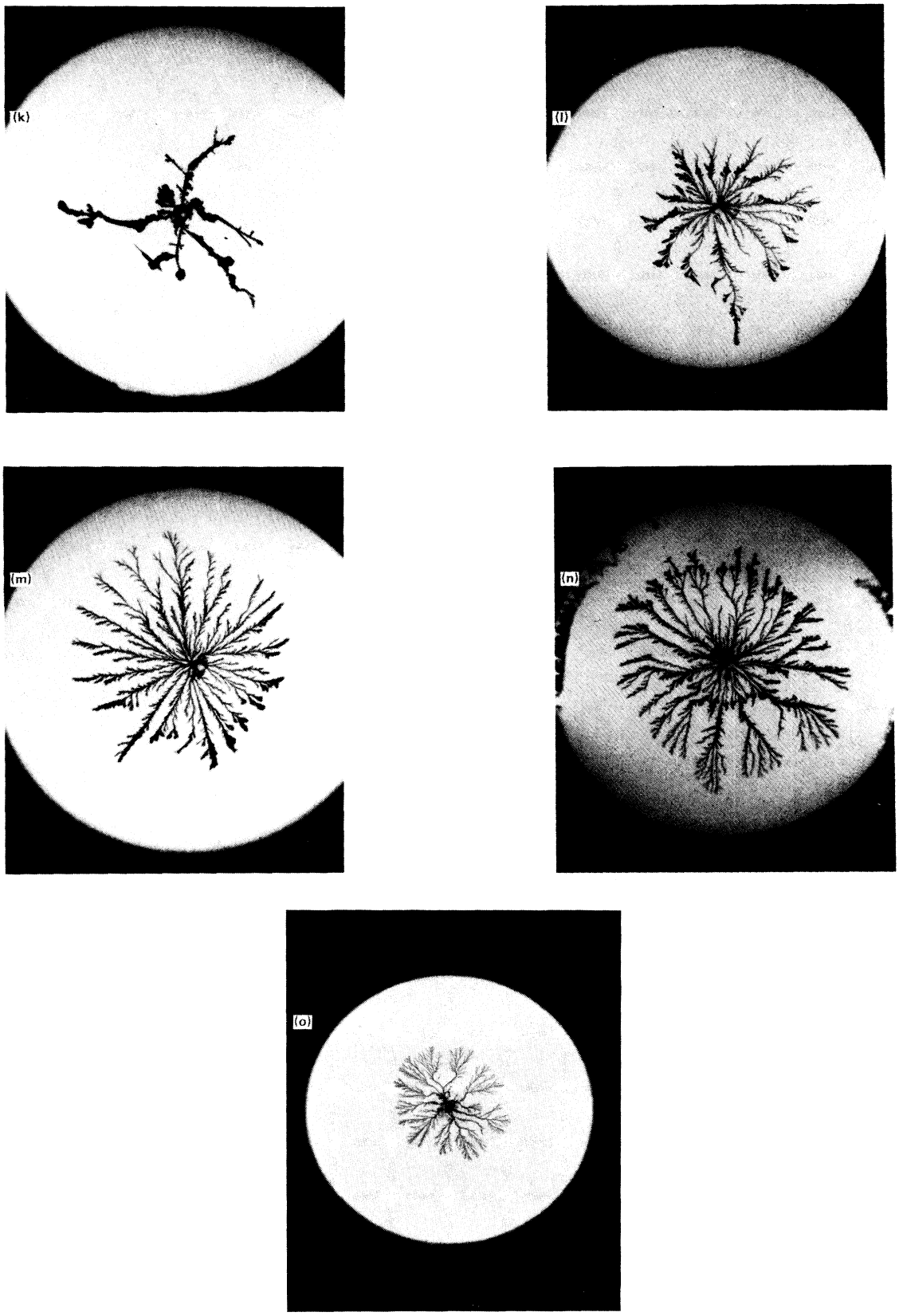

FIG. 1. (*Continued*).

dimensionality, $\bar{\mu}$, which measures the scaling of the shortest distance between two points. On a structure without loops, the chemical dimensionality provides an indirect measure of the spectral dimensionality. A particle (electron) diffusing on this object will exhibit scale-dependent diffusion such that in a time t it travels a mean radius $L_t \propto t^{1/(2+\theta)}$, where θ is the diffusion exponent related to $\bar{\mu}$, D, and d via $\theta=\bar{\mu}-d+D$. The spectral dimensionality is then given by $D_s=2D/(\bar{\mu}+2+D-d)$. Meakin and Stanley[11] calculate D_s in two dimensions and find $D_s=1.2\pm0.1$ or $\bar{\mu}=1.1\pm0.2$. Though it is true that $\bar{\mu}\simeq1$ is also true for a wire (and for percolation in two dimensions), it is important to note that the spectral dimensionality depends on both $\bar{\mu}$ and the fractal dimension D. A scale-dependent exponent of one does not imply a spectral dimension of one when the structure is manifestly not that of a wire. To obtain a spectral dimension of one from an object with fractal dimension 1.7, one would also require a value of 1.7 for $\bar{\mu}$ (i.e., $\bar{\mu}=D$).

Though many simulations have been preformed to determine fractional dimensionalities for this class of objects, the definitive theory of DLA does not exist. To make progress towards developing such a theory, it is necessary to consider the conditions which lead to diffusion-limited aggregation.

The random aggregation of particles by DLA is in fact the limiting case of a more general process of diffusion-*controlled* aggregation (DCA). In DCA, the flux of particles towards the growing surface is controlled (determined) by diffusion, but the free-particle concentration at the surface is nonzero as determined by the energetics of the deposition process.[13] In DLA, the surface concentration of aggregating particle falls to zero and the deposition rate is limited by diffusion alone. For example, in electrochemical deposition, the equilibrium concentration of particles near the growing surface is given by $c \propto \exp(-\alpha n e \Delta\phi/k_B T)$ where α is the barrier height for deposition, n is the number of electrons transferred per particle, and $\Delta\phi$ is the difference between the applied potential and the thermodynamic potential for deposition. Given a uniform "finite" concentration everywhere near the surface, deposition will proceed at sites which are kinetically and/or thermodynamically favored. For low values of $\alpha\Delta\phi$, the concentration gradient is sufficiently small that dendritic growth will not occur. For intermediate values, the deposition process is still partially controlled by the local thermodynamics, but the concentration gradient is large enough to overcome stabilizing processes like capillarity or the Gibbs-Thomson effect. At this point a planar electrode is known to become unstable.[14] Irregularities on the surface formed by, e.g., fluctuations, will propagate. In the absence of crystalline anisotropy, such tips or dendrites will grow normally from the surface and the angle between branches will be, on average, 90°. This preferred direction is fixed by the local concentration gradient. In the DCA regime, the gradient and finite concentration result in an effective force normal to the electrode surface. For very large values of $\alpha\Delta\phi$ the surface concentration is effectively zero and the deposition is (locally) DLA. The rate is limited only by diffusion and not by the kinetics or thermodynamics of a chemical reaction.

As pointed out by Brady and Ball,[5] deposition in an electrostatic potential gradient with high concentration at the growing surface may be analogous to DCA. However, if this gradient is not accompanied by a large concentration gradient, the conditions necessary for diffusion-limited aggregation may not exist (i.e., the concentration of aggregating particles at the growing surface will be nonzero). This may explain why experiments employing electrochemical deposition of metal ions in a potential gradient yield treelike structures at low deposition potential, but produce compact or dendritic structures at high potential where the deposition is field driven and the solution is stirred by solvent breakdown.

EXPERIMENTAL

Experiments to demonstrate the importance of migration were performed in a thin-layer cell constructed of two glass plates. On one plate a 10-μm layer of silver was evaporated except for a 1-in-diam circular region in the center. This region constitutes the electrochemical cell. A 10-mil hole was drilled through the center of the other plate and a silver wire was inserted, epoxied, and sheared flush with a razor blade. A second 10-mil hole was drilled 1 cm from the first to allow contact to the electrolyte with a micro-reference electrode. In the first experiment the electrolyte was $0.1M$ $AgNO_3$ aqueous with $0.1M$ KNO_3 as supporting electrolyte. In the second experiment the supporting electrolyte was omitted to eliminate screening of the electric field. In both cases the reference electrode was Ag/AgCl with $3M$ KNO_3. Samples were prepared at -0.5 V with respect to the Ag/AgCl reference electrode.

Polypyrrole is a conducting polymer which may be prepared by electrochemical oxidation of neutral pyrrole monomer in a variety of supporting electrolytes.[15] Samples of polypyrrole were prepared in a similar two-electrode thin-layer cell consisting of two glass plates separated by a 10-mil Kapton spacer and a 2000-Å gold counter electrode evaporated on one plate. A 10-mil hole was drilled through the center of the other plate and a 5-mil gold wire was inserted and sheared flush with a razor blade. The electrolyte was $0.1M$ silver tossylate in acetonitrile with $0.1M$ pyrrole. Since concentration dependence was not to be studied, the experiments were performed with only two electrodes. The applied voltage was varied between 0.8 V (the threshold for polymerization in this cell) and 6.0 V. Above approximately 5 V the current was insensitive to the potential, indicating the current was diffusion limited. These voltages do not reflect the actual half cell potential for polymerization because no reference electrode was used. The potentials are, therefore, characteristic of the particular cell configuration. However, even at the highest potentials the solvent (acetonitrile) is stable and no gas is evolved at either electrode (i.e., there is no stirring of the solution). The counter reaction is the deposition of silver and the structures visible on the counter electrode in Fig. 1(n) are silver dendrites. Note that the pyrrole experiment also differs from the metal deposition experiment described above in the boundary condition at the counter electrode. For the silver deposi-

tion, for each ion deposited, one is added to solution at the outer edge of the cell. In the case of the polymer, there is no source of pyrrole at the counter electrode.

To determine the fractal dimension of the structures produced, video images were acquired with a standard video camera. For growth kinetics measurements, these images were acquired, *in situ*, every ten seconds during polymerization. The maximum resolution of the images was 512×512. The data was digitized and processed with the IBM IAX image processing software. The correlation function was computed by setting a threshold intensity for the fractals, and producing a binary image. The two-dimensional autocorrelation function was computed (in the frequency domain) and radiometrically averaged. The inverse fast Fourier transform (FFT) of this function is identical to the density-density correlation function. This procedure is considerably faster than computing the all-points correlation function in the space domain. We denote the integrated density-density correlation function by $M(r)$. The slope of the log of this function with respect to $\log(r)$ determines the fractal dimension of an object.[6] In addition to measuring the fractal dimension, the branch angle distribution function was measured for each image. The angle between branches should give insight into the microscopic mechanisms at work when the compact electrode surface becomes unstable (see below). A photograph of the polymer was placed on a graphics tablet and three points (vertex and two branches) were recorded at hundreds of branch points chosen at random on the image. Since most angles correspond to side branches (as opposed to tip splitting), the measured angle is always the acute angle. There should, of course, exist a distribution of congruent angles between 90° and 180°. Each distribution was fitted to a Gaussian to compute the mean branch angle. We applied both of these techniques to polypyrrole prepared at different fixed potentials [Fig. 1(a)–1(o)].

RESULTS AND DISCUSSION

To demonstrate the effects of electric fields, silver aggregates were prepared under identical conditions except that in one case supporting electrolyte was added to provide some screening of the electric field. The applied potential was -0.5 V (with respect to the Ag/AgCl reference electrode) which is well below the potential for electrolysis of water (-0.7 V at pH7). At this potential, with supporting electrolyte, the current was diffusion limited but no stirring of the solution or gas evolution occurred. The aggregates produced are shown in Figs. 2(a) and 2(b). In Fig. 2(a) the field was screened and the deposition controlled by diffusion. The object is similar to a random aggregate and has fractal dimension 1.75 ± 0.03. The structure shown in Fig. 2(b) is obviously different (fractal dimension 1.81 ± 0.03). In this case the only screening is provided by the silver salt and silver ions are depleted near the growing surface. The voltage between the counter and working electrodes was measured and found to be approximately 1.1 V in the cell without supporting electrolyte and 1.0 V with supporting electrolyte. The difference reflects the difference in cell resistance for the different carrier concentrations. We wish to point out that the reference voltage of -0.5 V versus Ag/AgCl is a relatively high potential. For aqueous solutions, the half-cell potential at the active electrode can never exceed that for electrolysis of water even if the applied voltage is 20 V. In

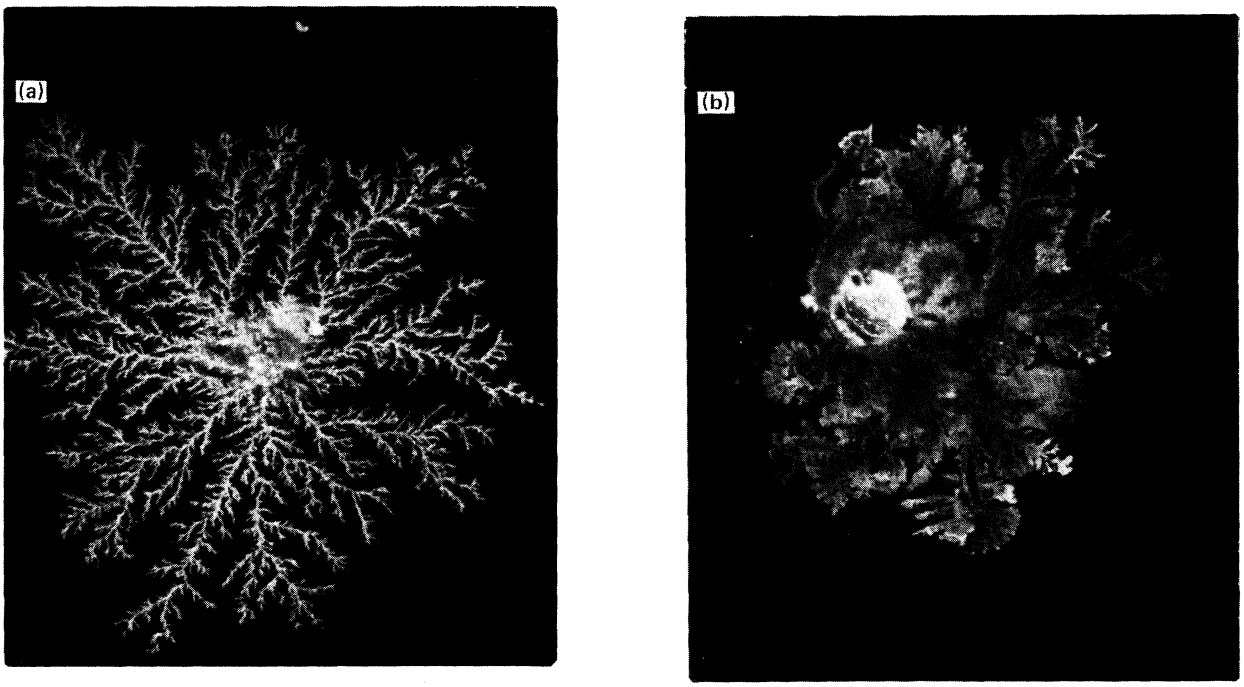

FIG. 2. (a) and (b) Aggregates of silver prepared with and without supporting electrolyte respectively (see text).

two recent Letters,[16,17] a pair of experiments were reported in which ionic species (zinc) were deposited without supporting electrolyte. No reference electrode was used and applied voltages exceeded that for electrolysis of water as evidenced by the evolution of gas. Variations in structure were studied as a function of applied voltage and concentration. The changes in structure observed in these experiments were affected by convection, stirring from gas evolution, diffusion, and migration (electric fields). The results were further complicated by the fact that without a reference electrode, the two-electrode applied potential is not a meaningful number when concentration is varied over orders of magnitude. In order to study the fundamental phenomena which govern diffusion-controlled aggregation, we chose to confine our studies to the deposition of neutral species under conditions which minimize effects other than diffusion. To avoid the necessity of a reference electrode, we used only one initial electrolyte concentration. The growth kinetics of a polymer aggregate prepared under diffusion-limited conditions are shown in Fig. 3. The figure shows the radial dependence of the integrated density-density correlation function, $M(r)$, at various stages of the growth. For R between 0.3 mm and 6.0 mm, the plot is linear with an exponent $D=1.74\pm0.03$. For small radii the exponent decreases to 1.42 ± 0.03. This may be an artifact of the digitization process since features smaller than a few pixels are lost and the structure approaches its topological dimension $D_t=1$.

The derivative of the normalized difference between successive curves in Fig. 3 is the probability of adding the next monomer unit at radius R. The peak of each distribution represents the radius of the aggregate at a given time. This data, plotted in the inset, reflects the width of the active growth zone as a function of time. When the peaks were each fit to a Gaussian, the widths increased with fractal size to the power 0.93 ± 0.05. The full width at half maximum (FWHM) of each peak was also measured without fitting to a particular function. The measured widths increased with R to the power 1.0 ± 0.04. Thus, the width of the active growth zone grows at the same rate as the fractal. This implies that only one length scale is required to characterize both the aggregate and its growth.[7–9]

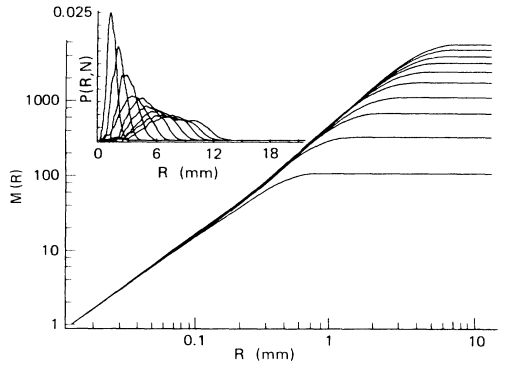

FIG. 3. The integrated density-density correlation function $M(r)$ vs r at successive times during DLP. The inset shows the width of the active growth zone for each stage of growth (see text).

To help visualize the growth process, some of the successive images used above were digitally summed, and the resulting intensities assigned different colors. The product (Fig. 4) is an image where different colors represent different stages of growth. The arms are somewhat thicker than those in the high contrast black and white photographs. This thickening is artificial and was introduced in the digitization process to make the picture more colorful.

As discussed above, since polypyrrole is a poor enough conductor (yet mechanically durable) it was possible to make scale-dependent conductivity measurements. Furthermore, since polypyrrole is an extrinsic semiconductor, charging effects[18] can be eliminated by measuring the scale-dependent conductivity at low-frequency ac (10 KHz). Below 1 MHz the resistance is constant. A series of probes were constructed with different contact separation (r). The contacts were made by rounding the tip of a fine gold wire with a torch. The tip was amalgamated to minimize contact resistance. Each probe was used to measure the resistance (ρ) of the sample at 10 random sites along and between branches. The results were averaged and plotted as $\log\rho$ versus $\log r$ (see Fig. 5). The scale-dependent conductivity exponent as determined by the slope of this data was 0.96 ± 0.04 with a correlation of

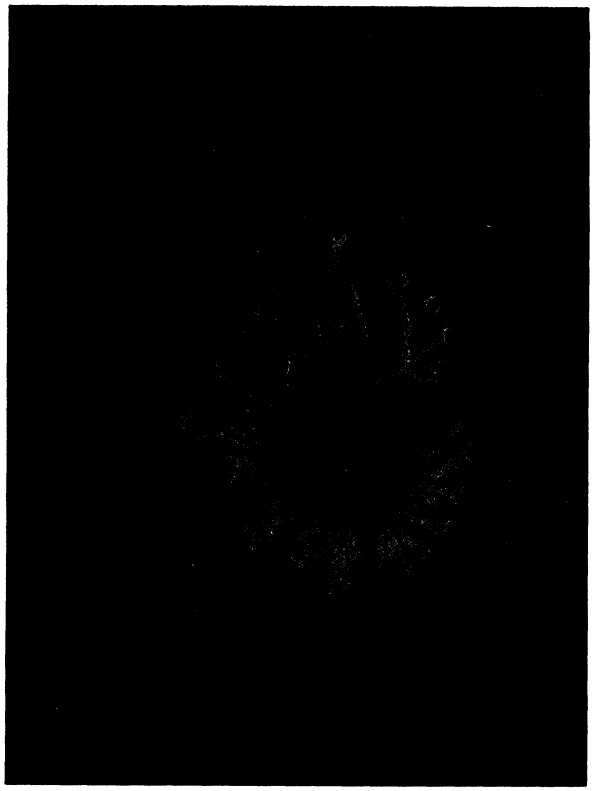

FIG. 4. Various stages of polymerization for a fractal. The colors are artificial.

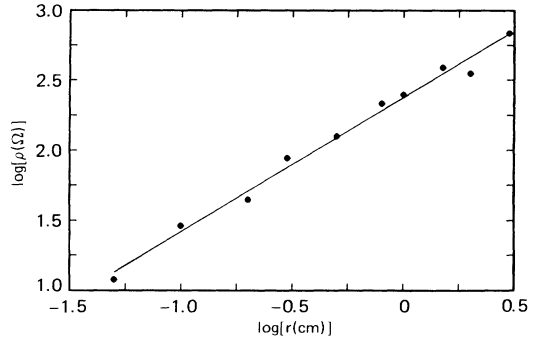

FIG. 5. The scale-dependent conductivity measured on an aggregate. The slope determines the chemical dimensionality of an aggregate.

0.994. For $D=1.7$, this implies $D_s=1.28\pm0.02$. A value of $D=1.65$, would imply $D_s=1.26\pm0.02$.

In Fig. 6 the voltage dependence of the averaged fractal dimension for a number of samples is shown. The data, plotted as D versus V, begins at a minimum voltage of 0.8 V which is near the threshold voltage for oxidation of pyrrole monomer in our cell. The most remarkable feature in the data is the sharp instability observed at about 1.5 V where the growth changes from compact [Fig. 1(a)] to dendritic [Fig. 1(h)]. At higher voltages a continuum of structures is observed as the growth becomes more irregular and the fractal dimension increases asymptotically to about 1.75. The left-hand side of this transition is predicted by the instability of a compact electrode growing into a sufficiently large gradient via DCA. A scanning electron micrograph (SEM) of the surface instability is shown in Fig. 7. Irregularities are evident on the surface. In the upper left-hand corner of the photograph, one of the irregularities continued to grow forming a branch which subsequently screened the interior surface. That the observed instability corresponds to the onset of dendritic growth is supported by the mean of the branch angle distribution function also plotted in Fig. 6. At 1.5

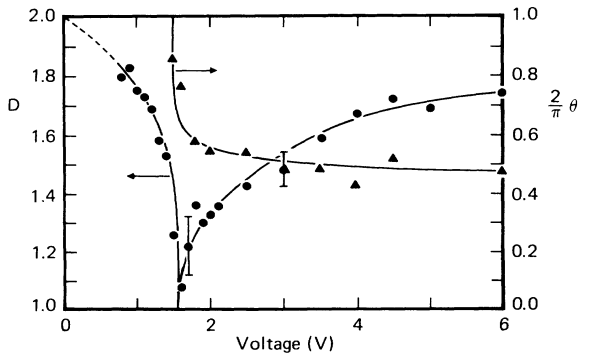

FIG. 6. The potential dependence of the structure plotted as D vs V. Also plotted is the potential dependence of the mean branch angle (right-hand axis). Note the growth instability near 1.5 V.

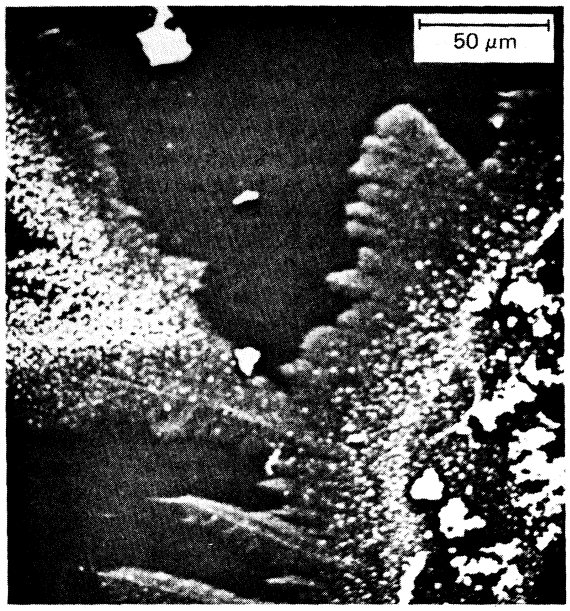

FIG. 7. An SEM of a pyrrole aggregate reveals that compact growth is unstable with respect to tip formation.

V the mean branch angle decreases from about 90° to 42°±7° at high voltage. Note that below 1.5 V the structure is compact and the branch angle is undefined. We also measured this distribution function for a diffusion-limited aggregate made by computer simulation (Ref. 2). Since the simulation is on a square lattice, all microscopic angles are 90°. However, when the aggregate is defocused, and the angles measured on scales greater than 10 lattice constants, the distribution was found to peak at 43°±6°. This agreement in no way implies that polypyrrole forms a square lattice. Transition electron micrographs (TEM's) of the polymer branches indicate the material formed is completely amorphous and should not exhibit crystalline anisotropy. Furthermore, we could conceive no convincing argument to explain the observed branch angle distribution from conjugation via α and β carbons on the pyrrole rings. We believe that the observed angle is characteristic of random aggregation with our boundary conditions. This does not rule out the possibility that the 45° branch angle observed in DLA simulations is due to the underlying lattice. Meakin *et al.*[19] have demonstrated that for simulations on a lattice, the lattice symmetry is preserved on large length scales. This can be explained by the fact that all particles are captured on lattice sites (i.e., it is possible to connect any two point on the fractal with a linear combination of lattice vectors). In real (crystalline) aggregates, the occurrence of new nucleation sites would destroy this long-range order and scaling would also be preserved for large dimensions.

The fact that this instability occurs in an amorphous material like polypyrrole suggests that the transition from diffusion-controlled aggregation to diffusion-limited aggregation is not, in general, a smooth one. The discontinuity in Fig. 6 indicates that the same instability which leads to dendritic growth precedes DLA even in the ab-

sence of crystalline anisotropy.

The structures obtained in the diffusion-limited regime are more dense than those obtained in DLA simulations. Similar structures have been reported by Sawada *et al.*[16] (who refer to some of their aggregates as "homogeneous"), and Grier *et al.*[17] The increase in density is probably due to the fact that before aggregation begins, the electrochemical cell is completely filled by a "gas" of particles, whereas in the simulations the space is empty except for a single random walker. In the limit of high initial particle concentration, the aggregate will resemble DLA on small scales. On large scales, however, the shape of the aggregate reflects the radial gradient. This effect may be more pronounced in cells where the aggregating particles are replaced at the counter electrode (so the concentration there increases) and the growth allowed to proceed into that region. In the case of the pyrrole aggregates, the total particle number is fixed and the concentration of particles decreases as the aggregate grows. This latter situation more closely resembles the models of DLA.

We believe that understanding both sides of the growth instability is critical to any complete theory of DLA. Since the random fractal is the limiting case of the diffusion-controlled aggregate, the correct theory of DCA should predict the transition from fractal to dendrite as well as dendrite to compact. The scale at which this transition occurs will be case dependent, but the occurrence of the transition should be universal. For example, aging in dielectrics exposed to high electric fields results in a transition from a uniform space charge density to a branched defect structure.[20,21] This transition from compact to dendritic space-charge distribution may reflect the same phenomenon which occurs in DCA, though the scale of the process is particular to the dielectric.

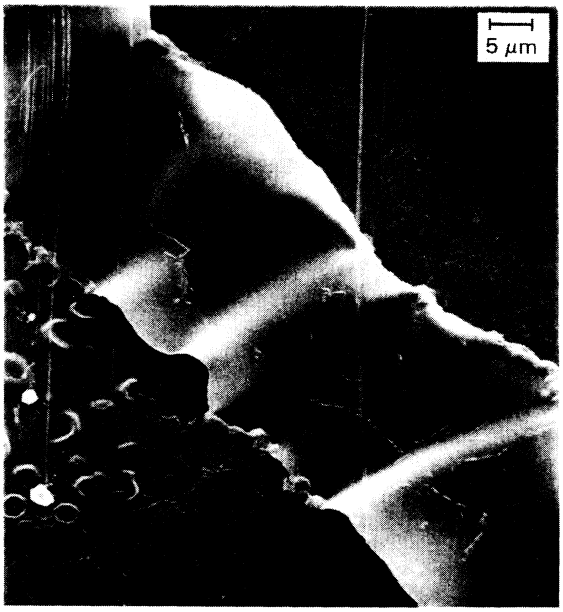

FIG. 8. This SEM of a single branch of a pyrrole aggregate prepared at 6.0 V with no spacer demonstrates that on some scale the material is compact (see text).

At voltages just above the transition in Fig. 6, the dendritic growth also becomes unstable for large samples. This effect manifests itself in some samples where, after reaching a critical length, dendrites (or arms) of the polymer stop growing and a compact structure grows on the tip. We believe this effect is due to the fact that polypyrrole is not highly conducting (0.1 Ω cm). When the *IR* drop along an "arm" is sufficient to decrease the potential at the growing tip below that for dendritic growth, the growth will become compact. If the arm subsequently thickens, the dendritic growth may proceed. This effect serves to increase the error in the data at potentials near the transition. At sufficiently high voltage it is possible to apply a potential large enough to sustain diffusion-limited growth (i.e., the current is voltage independent).

In the diffusion-limited regime, the pyrrole aggregates (like all real objects in nature) are compact on some scale. To study this, scanning electron micrographs were taken on aggregates prepared without the Kapton spacer. The cell thickness was then determined by the thickness of the gold counter electrode and any dust trapped between the glass plates. The SEM shown in Fig. 8 demonstrates that the arms are compact on length scales less than 10 μm, while the polymer thickness is on the order of 2000 Å. The fact that random aggregates can be produced at all using a system as complicated as a pyrrole polymerization demonstrates the generality and importance of random aggregation phenomenon.

CONCLUSION

In conclusion, we have demonstrated that electrochemical generation of a long-chain polymer results in the formation of a fractal structure when the rate of polymerization is limited by diffusion. While it is also possible to study DLA using electrochemical deposition of charged species (e.g., metal ions), our results demonstrate that effects other than diffusion dramatically affect the structure if care is not taken to screen the electric field.

We have studied the electrochemical polymerization of pyrrole under conditions which range from diffusion controlled to diffusion limited. At low oxidation potentials the structures were compact. At somewhat higher potentials a growth instability occurred and the aggregates became dendritic. The fractal dimension decreased sharply to 1. At higher potentials the fractal dimension increased asymptotically to 1.74 ± 0.03 as the polymerization becomes diffusion limited.

The fractal dimensionality for DLP was found to be 1.74 ± 0.03. The width of the active growth zone scaled with the fractal size to the power unity. The durability and relatively high resistivity of polypyrrole allowed direct determination of the spectral dimensionality[10,11] D_s of a fractal by scale-dependent conductivity measurement. The spectral dimension is found to be 1.28 ± 0.04 in good agreement with theoretical values for DLA. Thus, we have demonstrated the generalization of the concepts of DLA to the process of diffusion-limited polymerization. Both dynamic and static scaling properties expected for DLA are experimentally verified for DLP.

ACKNOWLEDGMENTS

We thank Farid Abraham and M. Flickner for many useful discussions.

[1]T. A. Witten, Jr. and L. M. Sander, Phys. Rev. Lett. **47**, 1400 (1981).

[2]See, e.g., in *Proceedings of the International Conference on Kinetics of Aggregation and Gellation,* edited by D. P. Landau and F. Family (North-Holland, Amsterdam, 1984).

[3]M. Matsushita, M. Sano, Y. Hayakawa, H. Honjo, and Y. Sawada, Phys. Rev. Lett. **53**, 286 (1984).

[4]S. R. Forrest and T. A. Witten, Jr., J. Phys. A **12**, L109 (1979).

[5]R. M. Brady and R. C. Ball, Nature **309**, 225 (1984).

[6]See, e.g., B. B. Mandelbrot, *The Fractal Geometry of Nature* (Freeman, San Fransisco, 1983).

[7]J. H. Kaufman, C. K. Baker, A. I. Nazzal, M. Flickner, O. R. Melroy, and A. Kapitulnik, Phys. Rev. Lett. **56**, 1932 (1986).

[8]M. Plischke and Z. Racz, Phys. Rev. Lett. **53**, 415 (1984).

[9]P. Meakin and L. M. Sander, Phys. Rev. Lett. **54**, 2053 (1985).

[10]T. A. Witten and Y. Kantor, Phys. Rev. B **30**, 4093 (1984).

[11]P. Meakin and H. E. Stanley, Phys. Rev. Lett. **51**, 1457 (1983).

[12]H. E. Stanley and A. Coniglio, Phys. Rev. B **29**, 522 (1984).

[13]See, e.g., A. J. Bard and L. R. Faulkner, *Electrochemical Methods, Fundamentals and Applications* (Wiley, New York, 1980), Chaps. 1, 4, and 6.

[14]W. W. Mullins and R. F. Sekerka, J. Appl. Phys. **34**, 323 (1963); **35**, 444 (1964).

[15]See, e.g., G. B. Street, *Handbook of Conducting Polymers,* edited by T. A. Skotheim (Marcel Dekker, New York, 1986), p. 265.

[16]Y. Sawada, A. Dougherty, and J. P. Gollub, Phys. Rev. Lett. **56**, 1260 (1986).

[17]D. Grier, E. Ben-Jacob, R. Clarke, and L. M. Sander, Phys. Rev. Lett. **56**, 1264 (1986).

[18]R. B. Laibowitz and Y. Gefen, Phys. Rev. Lett. **53**, 380 (1984).

[19]P. Meakin, R. C. Ball, and L. M. Sander, Annal. Israel. Phys. Soc. (to be published).

[20]L. Niemeyer, L. Pietronero, and H. J. Wiesmann, Phys. Rev. Lett. **52**, 1033 (1984).

[21]P. Pfluger, H. R. Zeller, and J. Bernasconi, Phys. Rev. Lett. **53**, 94 (1984).

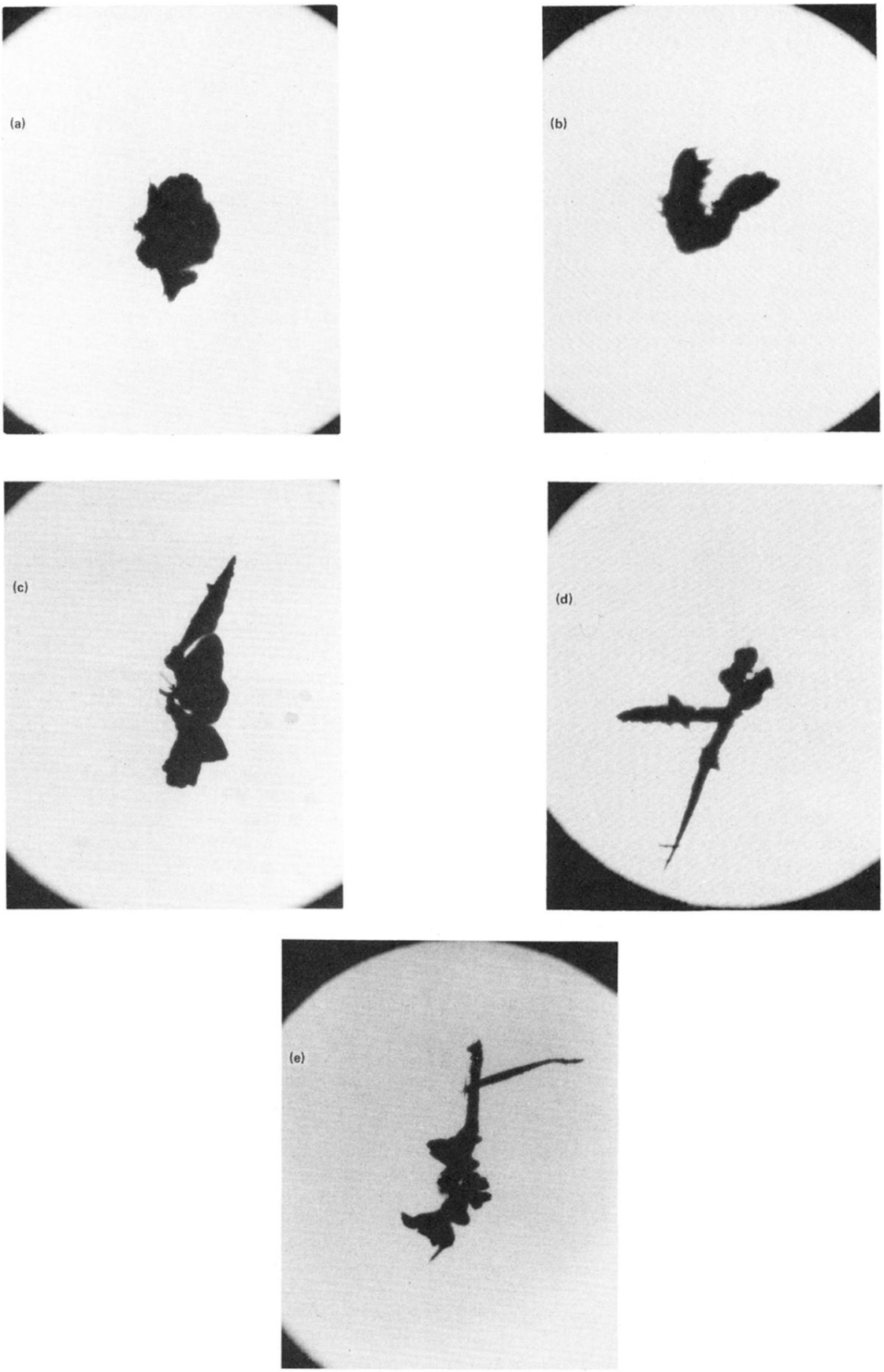

FIG. 1. (a)—(o) Aggregates of polypyrrole prepared via DCP at increasing potential: (a) = 0.8 V; (b) 0.9 V; (c) 1.0 V; (d) 1.1 V; (e) 1.2 V; (f) 1.3 V; (g) 1.4 V; (h) 1.5 V; (i) 1.6 V; (j) 1.8 V; (k) 2.0 V; (l) 3.0 V; (m) 4.0 V; (n) 4.5 V; (o) 6.0 V.

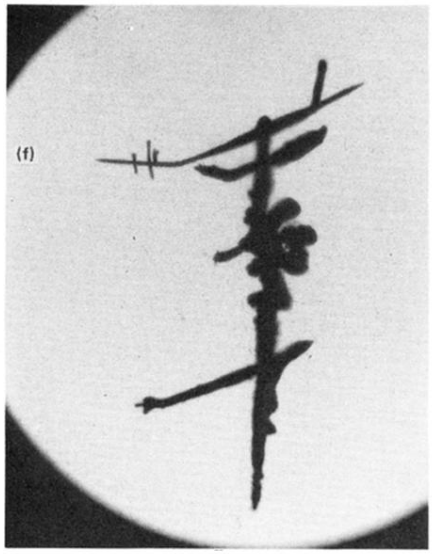

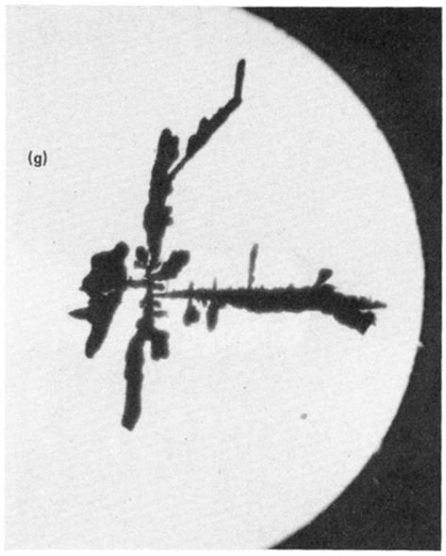

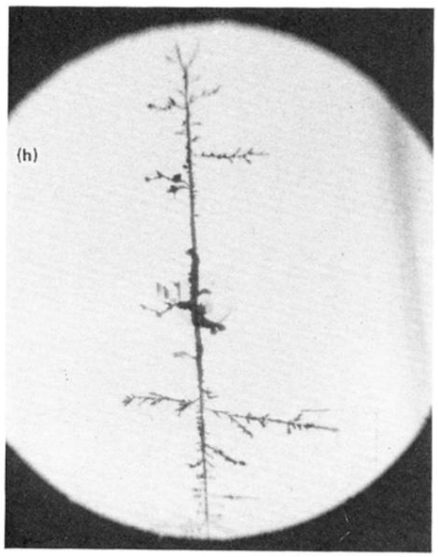

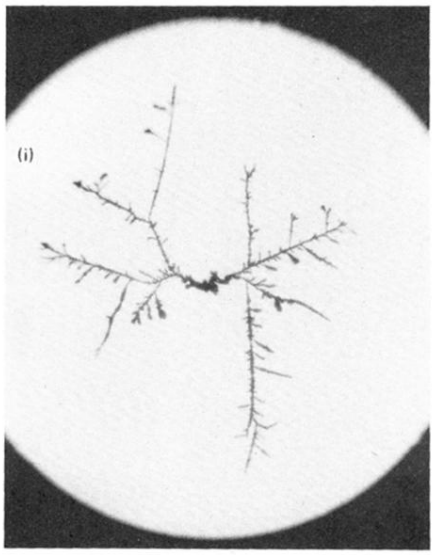

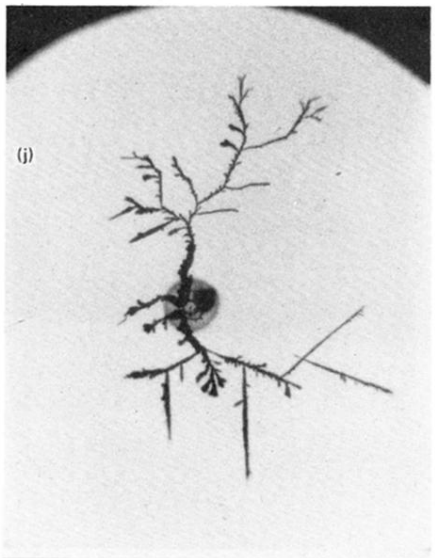

FIG. 1. (*Continued*).

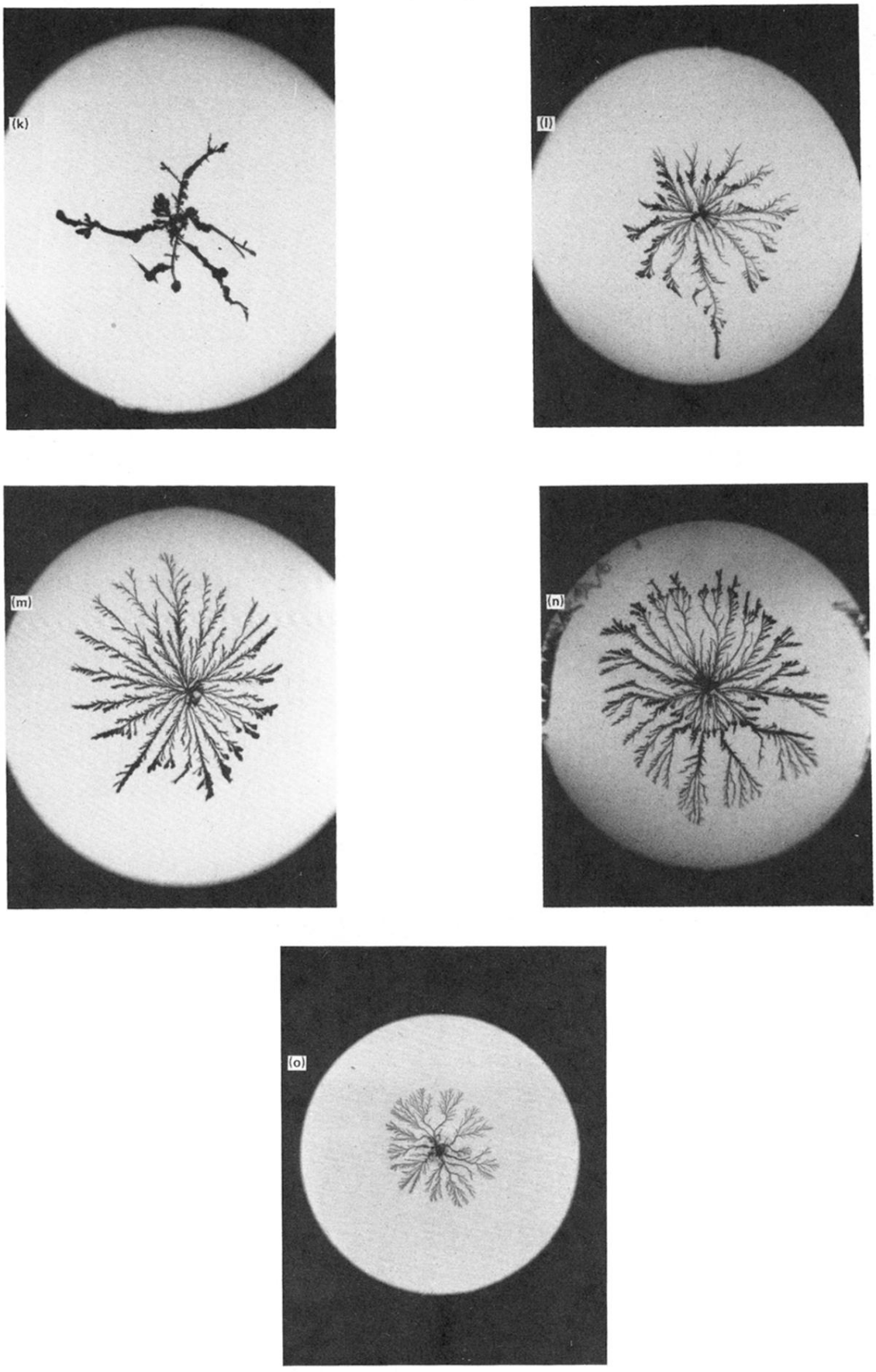

FIG. 1. (*Continued*).

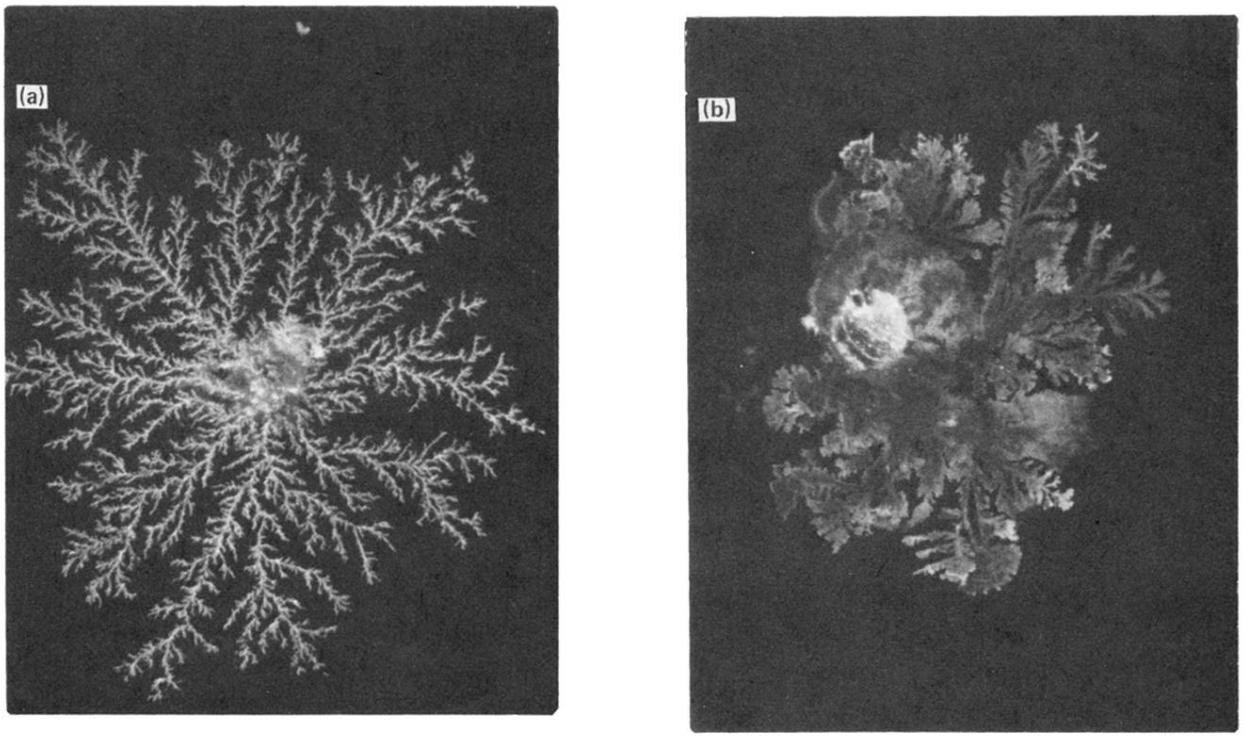

FIG. 2. (a) and (b) Aggregates of silver prepared with and without supporting electrolyte respectively (see text).

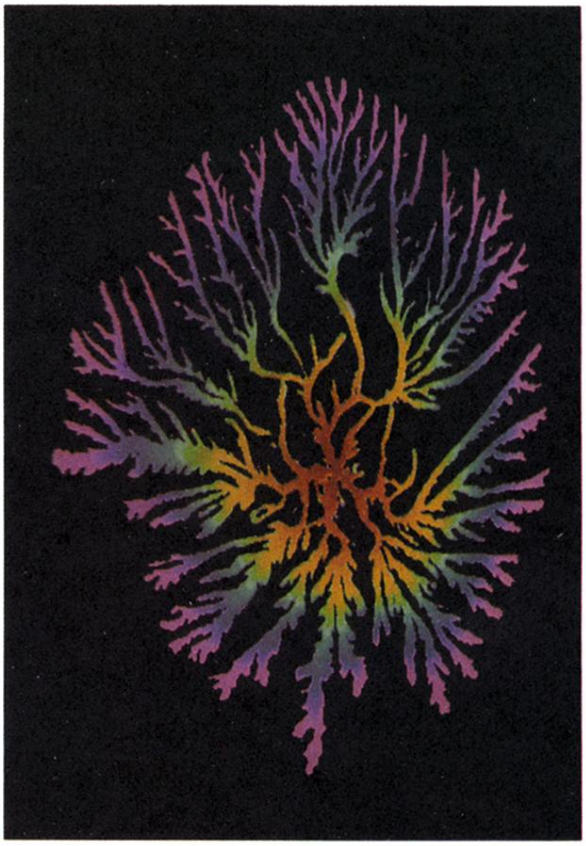

FIG. 4. Various stages of polymerization for a fractal. The colors are artificial.

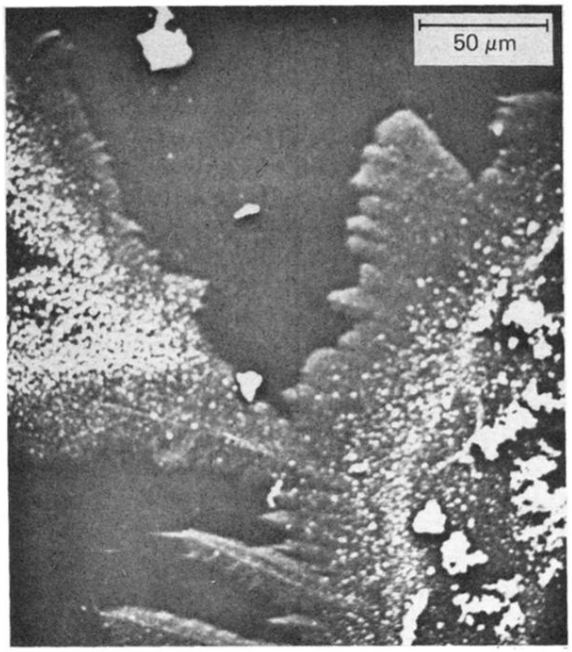

FIG. 7. An SEM of a pyrrole aggregate reveals that compact growth is unstable with respect to tip formation.

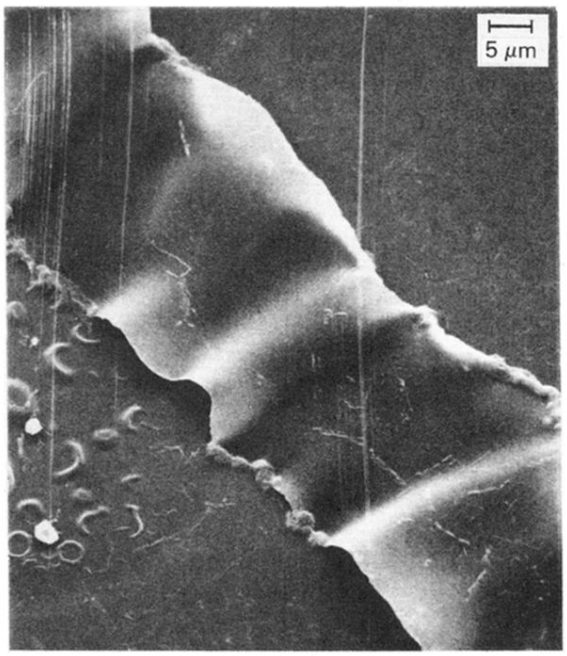

FIG. 8. This SEM of a single branch of a pyrrole aggregate prepared at 6.0 V with no spacer demonstrates that on some scale the material is compact (see text).